arXiv:1512.01198v1 [astro-ph.HE] 3 Dec 2015

A search for neutrino signal from dark matter annihilation in the center of the Milky Way with Baikal NT200

A.D. Avrorin[a], A.V. Avrorin[a], V.M. Aynutdinov[a], R. Bannasch[g], I.A. Belolaptikov[b], D.Yu. Bogorodsky[c], V.B. Brudanin[b], N.M. Budnev[c], I.A. Danilchenko[a], S.V. Demidov[a,*], G.V. Domogatsky[a], A.A. Doroshenko[a], A.N. Dyachok[c], Zh.-A.M. Dzhilkibaev[a], S.V. Fialkovsky[e], A.R. Gafarov[c], O.N. Gaponenko[a], K.V. Golubkov[a], T.I. Gress[c], Z. Honz[b], K.G. Kebkal[g], O.G. Kebkal[g], K.V. Konischev[b], A.V. Korobchenko[c], A.P. Koshechkin[a], F.K. Koshel[a], A.V. Kozhin[d], V.F. Kulepov[e], D.A. Kuleshov[a], V.I. Ljashuk[a], M.B. Milenin[e], R.A. Mirgazov[c], E.R. Osipova[d], A.I. Panfilov[a], L.V. Pan'kov[c], E.N. Pliskovsky[b], M.I. Rozanov[f], E.V. Rjabov[c], B.A. Shaybonov[b], A.A. Sheifler[a], M.D. Shelepov[a], A.V. Shkurihin[d], A.A. Smagina[b], O.V. Suvorova[a,*], V.A. Tabolenko[c], B.A. Tarashansky[c], S.A. Yakovlev[g], A.V. Zagorodnikov[c], V.A. Zhukov[a], V.L. Zurbanov[c]

[a] *Institute for Nuclear Research, 60th October Anniversary pr. 7A, Moscow 117312, Russia*
[b] *Joint Institute for Nuclear Research, Dubna 141980, Russia*
[c] *Irkutsk State University, Irkutsk 664003, Russia*
[d] *Skobeltsyn Institute of Nuclear Physics MSU, Moscow 119991, Russia*
[e] *Nizhni Novgorod State Technical University, Nizhni Novgorod 603950, Russia*
[f] *St. Petersburg State Marine University, St. Petersburg 190008, Russia*
[g] *EvoLogics GmbH, Berlin, Germany*

Abstract

We reanalyze dataset collected during 1998–2003 years by the low energy threshold (10 GeV) neutrino telescope NT200 in the lake Baikal in searches for neutrino signal from dark matter annihilations near the center of the Milky Way. Two different approaches are used in the present analysis: counting events in the cones around the direction towards the Galactic Center and the maximum likelihood method. We assume that the dark matter particles annihilate dominantly over one of the annihilation channels $b\bar{b}$, W^+W^-, $\tau^+\tau^-$, $\mu^+\mu^-$ or $\nu\bar{\nu}$. No significant excess of events towards the Galactic Center over expected background of atmospheric origin is found and we derive 90% CL upper limits on the annihilation cross section of dark matter.

Keywords:

1. Introduction

Today all cosmological and astrophysical observations are successfully explained within a paradigm of the standard cosmological model (ΛCDM) stating that most of the energy density of the Universe is stored in the dark energy or cosmological constant (Λ, about 68%) and non-baryonic cold dark matter (CDM, about 27%). Undoubted presence of the latter component is confirmed by measurements of galaxy rotation curves [1], weak gravitational lensing of distant objects like galaxy clusters [2], measurements of properties of cosmic microwave background [3, 4, 5], analysis of structure formation [6] and nucleosynthesis [7] (see also Ref. [8] for a review).

One of the most favorable ideas for explaining dark matter (DM) phenomena is Weakly Interacting Massive Particles or WIMPs [9]. In this scenario predicted by several classes of models of new physics [10, 11]

*Corresponding authors
Email addresses: demidov@ms2.inr.ac.ru (S.V. Demidov), suvorova@cpc.inr.ac.ru (O.V. Suvorova)

these particles are supposed to be in thermal equilibrium in the early Universe and can annihilate into Standard Model particles. But as the Universe was expanding and cooling down the annihilation processes ceased out and number density of dark matter particles became frozen out at some value which is determined by the annihilation cross section. Thus, at least in WIMP scenario one can expect some signal from dark matter annihilations towards directions of local overpopulation of these particles. The Galactic Center (GC) of the Milky Way is one of the such directions.

Two types of messengers from a DM annihilation signal in the Galactic Center, gamma rays and neutrinos, are expected to be detected by the telescopes . They are both originated in the same energy ranges (GeV–TeV for WIMPs) in decays of particles produced in kinematically allowed dark matter annihilation channels. Several analyses of diffuse gamma-rays from the FERMI-LAT dataset (pass 7) point out on an evidence for central and spatially extended excess toward the Galactic Center (GCE). (e.g. see Ref. [12] and references therein). Since the emissions from individual point sources like globular clusters and millisecond pulsars detected by the FERMI-LAT have been filtered in these analyses, the interpretations of the GCE as originating from DM annihilations in the MW halo were discussed [12]. In particular, the data support DM signal from annihilations either into $b\bar{b}$ channel with dark matter particle of the mass about 30–60 GeV or into $\tau^+\tau^-$ channel for the masses in 5–15 GeV range. The annihilation cross section is found to be about $10^{-26}\mathrm{cm}^3/\mathrm{s}$ which is close to its value predicted in the scenario of WIMPs annihilation in the early Universe. The latest analysis of the FERMI-LAT dataset (pass 8) [13] indicates some tension in consistency with dark matter interpretations of the GCE, related to dark matter density profile and value of local dark matter density.

The operating neutrino telescopes did not observe yet a signal from the dark matter annihilations in the GC in neutrino events over expected atmospheric neutrino background, see recent analyses from ANTARES [14], IceCube [15] and Super-Kamiokande [16]. In this paper we analyze the dataset of upward going muons produced by neutrinos in the lake Baikal and measured with NT200 telescope for a period between April of 1998 to February of 2003 and search for an excess in the directions near the GC. We focus on dark matter with masses from 30 GeV to 10 TeV annihilation dominantly over one of the following benchmark annihilation channels: $b\bar{b}$, W^+W^-, $\tau^+\tau^-$, $\mu^+\mu^-$ and flavor-symmetric neutrino channel $\nu\bar{\nu}$. Two independent analyses of the data are performed and consistent results are found. Finally, we obtain upper limits on dark matter annihilation cross section for these annihilation channels. Also we discuss influence of systematic uncertainties on the obtained results.

2. Experiment and data sample

The NT200 is a deep underwater neutrino telescope in the lake Baikal which has began data taking since 1996 year. This detector was the first who proved the method of study of high energy muons, which come from top or bottom hemisphere across a large volume of natural water, by recording their Cherenkov radiation [17]. Lake Baikal deep water is characterized by an absorption length of $L_{abs}(480\ nm) = 20 - 24$ m, scattering length of L_{sc} =30–70 m and strongly anisotropic scattering function with mean cosine of the scattering angle of 0.85–0.9. The Cherenkov light of relativistic particles is recorded at appropriate wavelengths by an array of optical modules (OMs) which are time-synchronized and energy-calibrated by artificial light pulses. At 1 km water depth, the muon flux from cosmic ray interactions in the upper atmosphere is about one million times higher than the flux of upward going muons initiated by neutrino interactions in water and rock below the array. Selection of clean neutrino event sample of true upward going muons is a major challenge which requires highly efficient rejection of misreconstructed downward moving muons.

The NT200 instrumentation volume encloses 100 Ktons being placed in the southern basin of the lake Baikal, at a distance of 3.5 km off the shore and at a depth of 1.1 km. In Fig. 1 the visibility over declinations for the NT200 site located at 51.83° of Northern latitude is shown. Here we account for its dead time when the detector had to be upgraded in the winter expeditions [18]. Note, that in April 2015 there has been deployed a new larger detector [19] operated now at this place as a demonstration cluster of about 2 Mton size for a future Gigaton volume detector [20]. Sensitivity of the future experiment to the DM annihilation signal from the GC has been discussed in Ref. [21].

The NT200 configurations, functional systems, calibration methods and software for muon track reconstruction have been described elsewhere [18, 22, 23, 24, 25, 26]. The detector consists of 192 optical modules arranged pairwise on 8 strings of 72 m length: seven peripheral strings and a central one. The distances between the strings are about 20 m. Each OM contains hybrid photodetector QUASAR-370, a photo multiplier tube (PMT) with 37-cm diameter. To suppress background from dark noise, the two PMTs of a pair are switched in coincidence within a time window of 15 ns.

Present analysis is based on data collected between April of 1998 and February of 2003, with in total 2.76 live years, and taken with the muon trigger. The trigger requires $N_{hit} \geq n$ within 500 ns, where *hit* refers to a pair of fired OMs coupled in a *channel*. Typically the value of n is set to 3 or 4. We use the same dataset and Monte Carlo (MC) sample as in Ref. [27]. The detector response to atmospheric muons and neutrinos has been obtained with MC simulations based on standard codes `CORSIKA` [28] and `MUM` [29] using the Bartol atmospheric ν flux [30]. To distinguish upward and downward going muons on a one-per-million mis-assignment level, a filter with several levels of quality cuts was developed for the atmospheric neutrino (ν_{at}) analysis [31]. The atmospheric muons which have been mis-reconstructed as upward-going particles are the main source of background in the search for neutrino induced upward-going muons. The offline filter which requires at least 6 hits on at least 3 strings ("6/3") selects about 40% of all triggered events. At this level the r.m.s. mismatch angle ψ between direction of the incoming muon and its reconstructed value is about 14.1° for the ν_{at}-sample. To get the best possible estimator for the direction, we use multiple start guesses for the χ^2 minimization [26]. For the final choice of the local minimum of χ^2 we use quality parameters which are not related to the time information. The quality cuts are applied to variables like the number of hit channels, $\chi^2/d.o.f.$, the probability of fired channels to have been hit or not and the actual position of the track with respect to the detector center. To improve the signal-to-background ratio we use only events with reconstructed zenith angle $\Theta > 100°$. All the cuts provide rejection factor for the

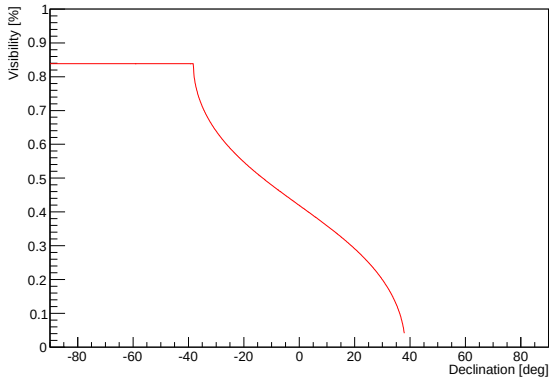

Figure 1: The NT200 visibility as a function of the declination

atmospheric muons of about 10^{-7}, resulting in the neutrino energy threshold of about 10 GeV, dispersion of 4.5° for the distribution of mismatch angles and median value 2.5° [26]. In Fig. 2 we show arrival directions of reconstructed muons in galactic coordinates and cones around the GC with opening angles 20°, 5° and 2.5° containing 31, 2 and 2 observed events, respectively. In the next Section we discuss expected signal from dark matter annihilations in our Galaxy and background from atmospheric neutrino.

3. Signal and background

Neutrino flux at the Earth from the dark matter annihilations in the Galactic Center from a particular direction has the following form

$$\frac{d\phi_\nu}{dE_\nu d\Omega} = \frac{\langle \sigma_a v \rangle}{2} \, J_a(\psi) \, \frac{R_0 \rho_0^2}{4\pi m_{DM}^2} \, \frac{dN_\nu}{dE_\nu}, \tag{1}$$

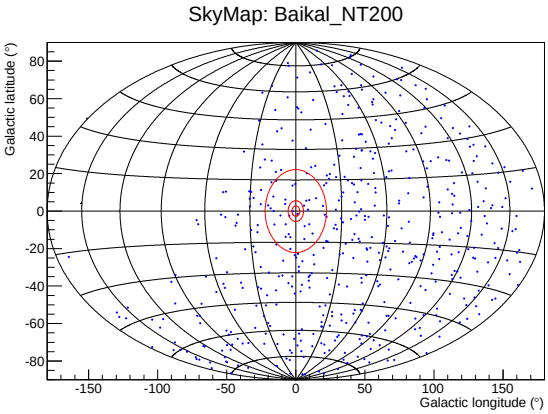

Figure 2: The NT200 sample of neutrino events in galactic coordinates

where $\langle\sigma_a v\rangle$ is annihilation cross section averaged over velocity distribution of dark matter particles at present epoch and dN_ν/dE_ν is (anti)neutrino energy spectrum. The astrophysical factor $J_a(\psi)$ can be parametrized as a function of angular distance ψ from the GC to the chosen direction and has the form

$$J_a(\psi) = \int_0^{l_{max}} \frac{dl}{R_0} \frac{\rho^2\left(\sqrt{R_0^2 - 2rR_0\cos\psi + r^2}\right)}{\rho_0^2}. \tag{2}$$

Here R_0 is the distance from the GC to the Solar System, ρ_0 is the local dark matter density and integration goes along line-of-sight till l_{max} which is much larger than the size of the Milky Way. Several different models are used to describe the dark matter density distribution of our Galaxy, see e.g. Refs. [32, 33, 34, 35, 36]. Numerical N-body simulations [37] show that dark matter form an almost spherical halo. Simulations without baryons predict cuspy profiles. However, inclusion of baryons can change these conclusions and N-body simulations being limited in number of particles can not resolve small area around the center of galaxy, so the main uncertainty in the profile comes from this region. At the same time the signal from annihilations is proportional to the square of dark matter density, see Eq. (1). So, this part of astrophysical input is the main theoretical uncertainty for signal from DM annihilations in the Galaxy. Direct observational data of the Milky Way can not resolve this uncertainty, because the part of our Galaxy within the Solar System circle is dominated by baryons, so the influence of the dark matter within this circle on motion of astrophysical objects is small. Even local dark matter density is known with a large uncertainty 0.2–0.6 GeV·cm^{-3}. Moreover, one can not exclude a possibility that dark matter can form clumps in our Galaxy and then signal from a particular directions can be increased by the presence of a clump along line-of-sight [38]. We will present the final results for Navarro-Frenk-White (NFW) [32, 33] and compare them with more cuspy Moore [35] profile and cored Burkert [36] profile. All these profiles can be described as follows

$$\rho(r) = \frac{\rho_*}{\left(\delta + \frac{r}{r_*}\right)^\gamma \left[1 + \left(\frac{r}{r_s}\right)^\alpha\right]^{(\beta-\gamma)/\alpha}} \tag{3}$$

with parameters presented in Table 1.

Neutrino energy spectra entering Eq. (1) are determined by a particular theoretical model. In a model independent approach followed in the present study it is assumed that the dark matter particles annihilate over particular annihilation channel with 100% branching ratio. We use $b\bar{b}$, $\tau^+\tau^-$, $\mu^+\mu^-$, W^+W^- channels as well as $\nu\bar{\nu} \equiv \frac{1}{3}(\nu_e\bar{\nu}_e + \nu_\mu\bar{\nu}_\mu + \nu_\tau\bar{\nu}_\tau)$ which is flavor symmetric combination of (almost) monochromatic neutrino. We consider the masses of dark matter particles from 30 GeV to 10 TeV. For the energy spectra of these annihilation channels we use the results of Ref. [39] which include electroweak corrections important

Model	α	β	γ	δ	r_*, kpc	ρ_*, GeV/cm^3
NFW	1	3	1	0	20	0.3
Burkert	2	3	1	1	9.26	1.88
Moore	1.5	3	1.5	0	28	0.27

Table 1: Parameters of DM density profiles.

for large masses of dark matter particles. After propagation over astrophysically large distances neutrinos from the GC arrive at the Earth as mass states and we use the following set [40] of oscillation parameters: $\Delta m^2_{21} = 7.6{\cdot}10^{-5}$ eV^2, $\Delta m^2_{31} = 2.48{\cdot}10^{-3}$ eV^2, $\delta_{CP} = 0$, $\sin^2\theta_{12} = 0.323$, $\sin^2\theta_{23} = 0.567$, $\sin^2\theta_{13} = 0.0234$ to calculate muon (anti)neutrino energy spectrum. We simulate neutrino propagation through the Earth to the detector level as described in [41]. Final neutrino energy spectra are presented in Fig. 3 as an example for $m_{DM} = 500$ GeV[1].

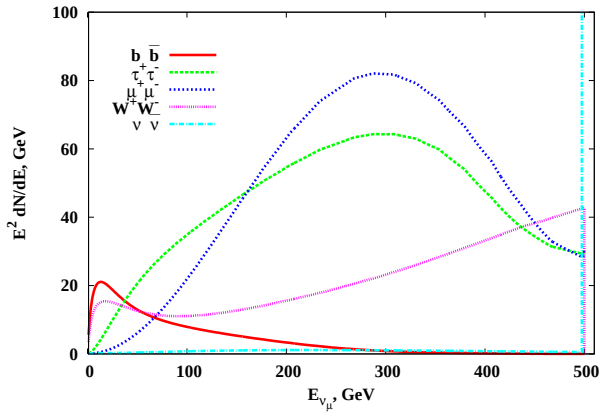

Figure 3: Neutrino ν_μ energy spectra at the Earth for $m_{DM} = 500$ GeV.

Expected angular distributions of reconstructed signal events (muons), was obtained by MC simulations. The angular spread of the signal is determined by the behaviour of the astrophysical factor $J_a(\psi)$ for a DM density profile, angular distribution of muons from CC interactions of neutrinos for a particular annihilation channel as well as angular resolution of the telescope. The latter has been taken into account by additionally smearing the signal according to the distribution of mismatch angles obtained with MC (instead of Gaussian distribution with dispersion equal to the angular resolution). Expected reconstructed angular distributions of the signal are presented in Fig. 4 for two opposite cases: the softest ($b\bar{b}$, $m_{DM} = 30$ GeV) and the hardest ($\nu\bar{\nu}$, $m_{DM} = 10$ TeV) neutrino energy spectra for NFW density profile.

The background for the process in question is dominated by upgoing atmospheric neutrinos. To avoid large systematic errors, typically resulted from MC simulations, in the following analysis we use the expected background which is estimated from the data using their scrambling by randomization of right ascension of the events. The form of the background obtained in this way is shown in Fig. 5 by blue histogram. In addition to the scrambling we introduce a correction to overall normalization of this background distribution by fitting it with the real data outside the region of expected signal contamination: we do it for $\psi > 60°$. For cross checking we use another procedure to obtain the shape of the background angular distribution. Namely we simulate the reconstructed atmospheric neutrino angular distribution taking into account the

[1] For the case of $\nu\bar{\nu}$ channel an unphysical width was introduced in Ref. [39]. We changed these spectra back to their physical width conserving their normalization.

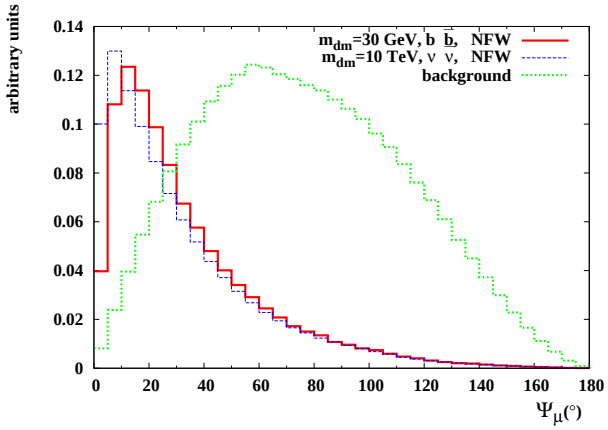

Figure 4: Expected reconstructed signal and background angular distributions.

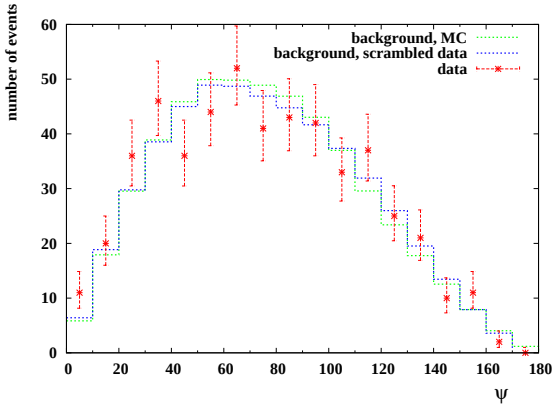

Figure 5: Data with statistical errors (red) in comparison with background obtained using scrambling the data (blue) and from Monte-Carlo (green) angular distributions.

visibility and imposing conditions on selected events. Again we fit obtained shape with the date in the region $\psi > 60^\circ$. The comparison between two different background is presented in Fig. 5 along with the data angular distribution.

By comparison of obtained angular distributions of signal and background with the data presented in Figs. 5 and 4 we see that there is a small excess in number of observed events toward the GC. Below we estimate statistical significance of the excess and obtain upper limits on number of signal events for each particular DM mass and annihilation channel. Concerning the cones shown in Fig. 2 the numbers of the expected background events (observed events) inside them are 25.1 (31), 1.63 (2) and 0.42 (2).

4. Data analyses

In this section we describe two different methods to analyze the data and to look for neutrino signal from dark matter annihilations in the GC. Expected signal and background have different energy and angular distribution. Here we can use only angular information of the reconstructed events.

4.1. Method A: Optimization of the cone size

For analysis A we choose a cone around the direction towards the GC with half-open angle Ψ and thus obtain a counting experiment with expected number of signal $N_S(\Psi)$ and background $N_B(\Psi)$ as well

as observed $N_{obs}(\Psi)$ number of events. The size of the cone is optimized by choosing maximal value for signal-to-noise ratio. Namely following to the MRF approach [42] we construct the quantity

$$\frac{S}{N} \equiv \frac{\bar{N}_S^{90}(\Psi)}{\sqrt{N_B(\Psi)}}, \tag{4}$$

where $\bar{N}_S^{90}(\Psi)$ is 90% CL upper limit on the number of signal neutrino events inside given cone of the size Ψ averaged over number of observed events with Poisson distribution under background only hypothesis. Optimal values of Ψ for different dark matter masses and annihilation channels are presented in Fig. 6. They

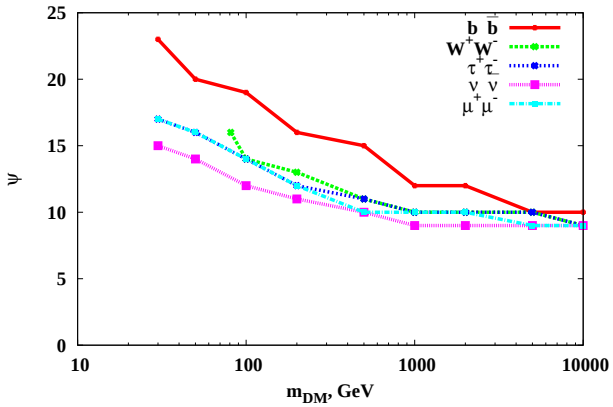

Figure 6: Optimal values of cone half-angles for different dark matter masses and annihilation channels.

vary from 9° for channels with hard ν spectra to about 23° for annihilations with soft neutrinos. Obtained large values are due to a considerable angular spread of neutrino signal (for NFW profile) as well due to a broad distribution of the reconstructed mismatch angles.

Inside the cones of optimal size we set upper limits on number of signal events N_S^{90} for a given DM mass and annihilation channel by using expected background distribution toward the GC. We apply TRolke class [43] in ROOT [44] to get the numbers, as well with included systematic uncertainties to be discussed in the next Section.

These upper limits are transformed into the upper limits on the dark matter annihilation cross section by using the expression for expected number of signal events from the GC direction for a live time T of observation inside given cone

$$N(\Psi) = T\frac{\langle\sigma_a v\rangle R_0\rho_0^2}{8\pi m_{DM}^2} J_{a,\Delta\Omega} S^{eff} \int_{E_{th}}^{m_{DM}} dE \frac{dN_\nu}{dE_\nu}. \tag{5}$$

Here S^{eff} is an effective area of the telescope averaged over neutrino energy spectrum for a particular annihilation channel

$$S^{eff} = \frac{\int dE S(E)\frac{dN_\nu}{dE_\nu}}{\int dE \frac{dN_\nu}{dE_\nu}} \tag{6}$$

within energy range from neutrino energy threshold E_{th} to DM mass m_{DM} and with implied sum over neutrino and antineutrino contributions. The neutrino effective area $S^i(E_{th}, E_\nu)$ of the NT200 for a given configuration is a product of the efficiency ϵ_ν^i of muon reconstruction i.e. the ratio of two-dimensional angular-energy distributions of reconstructed events to simulated neutrinos, and neutrino impact area defined by MC generated volumes V_{MC}^i and length of charged current (CC) neutrino interactions in water depending neutrino energy E_ν:

$$S^i(E_{th}, E_\nu, d\Omega) = V_{MC}^i \times N_A \times \rho \times \sigma^{CC}(E_\nu) \times \epsilon_\nu^i(E_{th}, E_\nu, d\Omega), \tag{7}$$

where $i = 1, ..., 12$ refers to twelve NT200 configurations operated in 1998-2003. The efficiency $\epsilon^i_\nu(E_{th}, E_\nu, d\Omega)$ is convoluted with a visible zenith track of the GC and thus $S(E_{th}, E_\nu)$ is entering into Eq.(7). The mean value of the generated volumes is $V_{MC} = 4.406 \times 10^{14}\text{cm}^3$. The value N_A is the Avogadro number, ρ the medium density (rock or water), σ^{CC} the neutrino-nucleon cross section in CC interactions. We omit the exponential attenuation of the neutrino flux in the Earth in Eq.(7) since the shadowing effect is very weak for energies less than 10 TeV. The total effective area is obtained by averaging $S^i(E_{th}, E_\nu)$ with fractions of time during which a particular i-th configuration of the telescope was at work. The NT200 effective areas

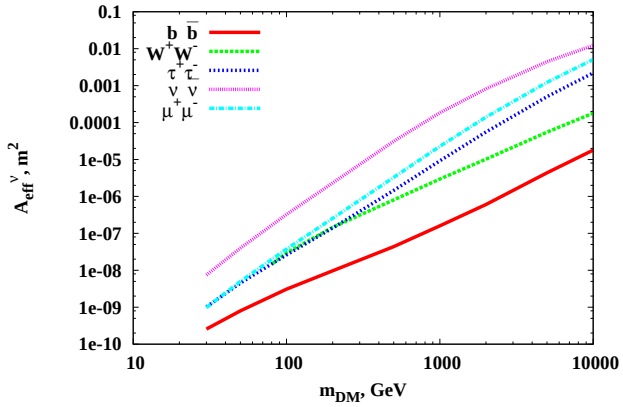

Figure 7: Effective area as a function of the mass m_{DM} of the DM particle for different annihilation channels.

versus masses of dark matter particle for particular annihilation channels are shown in Fig. 7. The softest neutrino spectrum in $b\bar{b}$ channel has the lowest effective area, while the largest area is for hard pure neutrino channel. The quantity $J_{a,\Delta\Omega}$ in Eq. (7) is obtained by integrating the astrophysical factor $J_a(\psi)$ over the search region with visibility $\epsilon(\psi, \phi)$ as follows

$$J_{a,\Delta\Omega} = \int d(cos\psi)d\phi J_a(\psi)\epsilon(\psi, \phi). \tag{8}$$

The upper limits for dark matter annihilation cross section are set by inverting the formula (5) with respect to $\langle\sigma_a v\rangle$ for given annihilation channel. Obtained results with included systematic uncertainties are shown in Fig. 8 by dashed lines in comparison with those obtained with method B (see next subsection).

4.2. Method B: Maximum likelihood ratio

In the analysis B we construct likelihood function and use more detailed information about angular distributions of signal and background. In this case we choose sufficiently large signal region $\psi < 40°$ for counting events and disregard another part as it is expected to be dominated by background. Let $f_S(\psi)$ and $f_B(\psi)$ be expected signal and background angular distribution functions normalized in the search region. In case of nonzero number of signal events one expects the data will be distributed according to

$$f(\psi, N_S, N_B) = \frac{1}{N_S + N_B}\left(N_S f_S(\psi) + N_B f_B(\psi)\right). \tag{9}$$

The likelihood function is then constructed as a product of probability distribution functions for obtained events

$$\mathcal{L}(N_S) = \frac{(N_B + N_S)^n}{n!}\mathrm{e}^{-(N_B+N_S)}\prod_{i=1}^{n} f(\psi_i, N_B, N_S) \tag{10}$$

with a multiplier with the form of Poisson distribution accounting for fluctuations in total number of events. Here n is the number of observed events in the search region. Systematic uncertainties for both signal

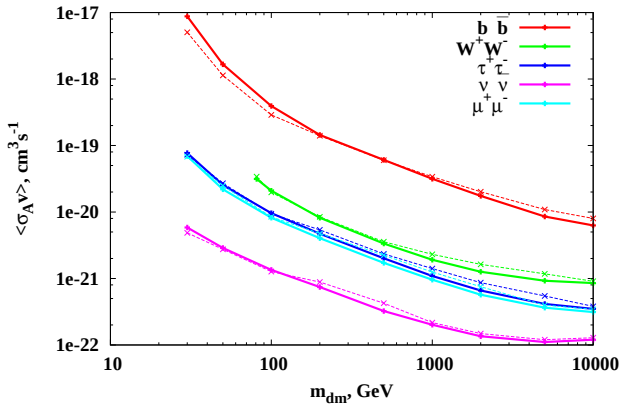

Figure 8: 90% CL upper limits for annihilation cross section for methods A (dashed) and B (solid) assuming NFW density profile.

and background are incorporated in the likelihood function as nuisance parameters $\theta \equiv \{\epsilon_S, \epsilon_B\}$ which are modeled by Gaussian distributions. They modify the probability likelihood function as follows

$$\mathcal{L}(N_S, \epsilon_S, \epsilon_B) = \mathcal{N}\frac{(\epsilon_B N_B + \epsilon_S N_S)^n}{n!}\mathrm{e}^{-(\epsilon_B N_B + \epsilon_S N_S) - \frac{(\epsilon_S - 1)^2}{2\sigma_S^2} - \frac{(\epsilon_B - 1)^2}{2\sigma_B^2}} \prod_{i=1}^{n} f(\psi_i, \epsilon_B N_B, \epsilon_S N_S), \qquad (11)$$

where σ_S, σ_B are systematic uncertainties which will be discussed in the next Section and $\mathcal{N}$ is a normalization factor. Then, the following profile likelihood

$$\lambda(N_S) = -2\ln\frac{\mathcal{L}(N_S, \hat{\hat{\theta}}(N_S))}{\mathcal{L}(\hat{N_S}, \hat{\theta})} \qquad (12)$$

is used to obtain upper limits on number of signal events. Here $\hat{N_S}$ and $\hat{\theta}$ are values which give absolute maximum to the likelihood probability function, while $\hat{\hat{\theta}}(N_S)$ denotes the values of maximum of the likelihood at fixed value of N_S. Number of observed events inside the search region $\psi < 40$ equals 113, that is sufficiently large for the quantity $\lambda(N_S)$ to be distributed according to χ^2 distribution with one degree of freedom according to Wilks theorem [45, 46]. We have checked out this numerically by running 10000 pseudo-experiments. Then we obtained the upper limits on number of signal events in the search region at 90% CL by solving the equation $\lambda(N_S^{90}) = 2.71$ [46].

To set the upper limits on dark matter annihilation cross section in a particular channel for a given DM mass, we use the same inversion of the formula (5) as in the description of the analysis A. Numerical values of the upper limits on the annihilation cross section obtained at 90% CL with the method B are presented in Table 2 and in Fig. 8 (solid lines) .

5. Results and discussion

We summarize our results for annihilation cross section for different channels in plots shown Figs. 8–11 comparing limits, obtained using methods A and B, with other experiments. Firstly, we have obtained the consistent results of both analyses. In Fig. 8 the upper limits at 90% CL on annihilation cross sections of a DM particle into five particular channels obtained with cone half-angle analysis (dashed lines) and with the method of maximum likelihood ratio (solid lines) are shown. Somewhat stronger upper limits are obtained with likelihood analysis for most of the chosen dark matter masses and annihilation channels.

m_{DM}, GeV	$\langle\sigma_A v\rangle$, 10^{-21}cm^3/s, NFW, method B				
	$b\bar{b}$	W^+W^-	$\tau^+\tau^-$	$\mu^+\mu^-$	$\nu\bar{\nu}$
30	8770	–	76.9	69.3	5.86
50	1660	–	25.4	21.9	2.88
100	392	20.9	9.61	8.21	1.35
200	144	8.19	4.71	4.04	0.742
500	60.9	3.35	2.01	1.72	0.324
1000	31.6	1.91	1.09	0.957	0.201
2000	17.5	1.26	0.659	0.57	0.135
5000	8.55	0.926	0.414	0.364	0.111
10000	6.28	0.852	0.349	0.313	0.120

Table 2: 90% CL upper limits on annihilation cross section for NFW dark matter density profiles; analyses B

We run pseudo-experiments with expected background only distribution to estimate the NT200 sensitivity to a DM signal in the GC from annihilation for opposite cases of soft $b\bar{b}$ and hard $\nu\bar{\nu}$ neutrino spectra. Expected sensitivities at 90% CL are presented in Fig. 9 together with the upper limits obtained by method B. Colored bands in these Figures represent 68% (red) and 95% (blue) quantiles. The observed upper limits

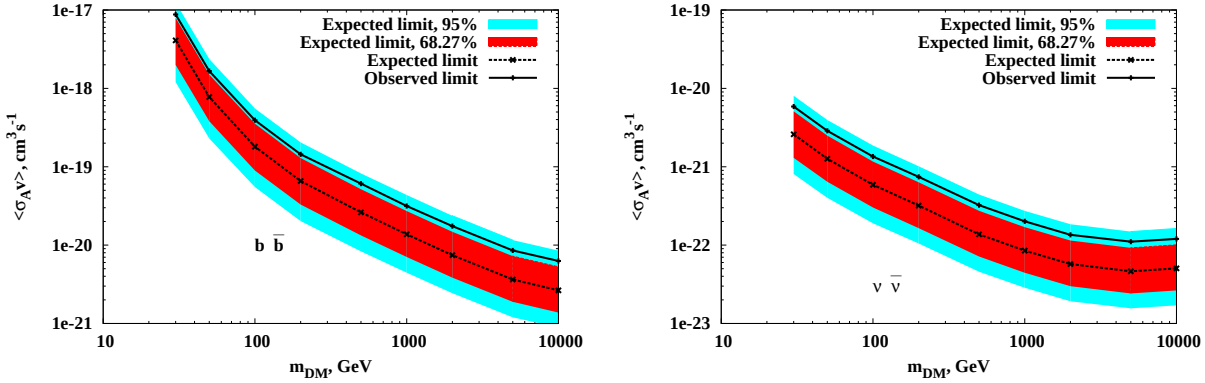

Figure 9: The upper limits on annihilation cross section versus a DM mass for channels $b\bar{b}$ (left) and $\nu\bar{\nu}$ (right) at 90% CL (black, solid) and the expected sensitivities (black, dashed) within its 1σ (red band) and 2σ (blue band) levels of statistical uncertainty.

are weaker as compared to the mean values of the sensitivity, because of a small excess of events in the direction towards the GC. This excess can be attributed to a statistical fluctuation of the background only expectation within less than 2σ level. Calculating TS of this excess under background only hypothesis we find values $5.8 - 6.6$ without any systematic errors depending on annihilation channels. Inclusion of experimental and theoretical systematic uncertainties (but not from astrophysics) results in decrease of these values to $1.4 - 1.6$.

Neutrino telescopes are most sensitive to pure neutrino annihilation channels. In Fig. 10 we show NT200 results (red line) for $\nu\bar{\nu}$ channel along with limits from other neutrino experiments, the ANTARES [14], IceCube[15], Super-Kamiokande [16] and also 1 year sensitivity of 12 clusters of Baikal-GVD project [21] to dark matter annihilation signal in the GC. Other annihilation channels can be probed also by gamma-telescopes. In Fig. 11 we compare the upper limits at 90% CL on $\tau^+\tau^-$ annihilation cross section obtained with NT200 dataset and other experiments including results by FERMI [49] (dwarf galaxies, DES), VERITAS [50] (four dwarf galaxies), MAGIC [51] (Segue 1), HESS [52] (dwarf galaxies) , IceCube [53] (GC and

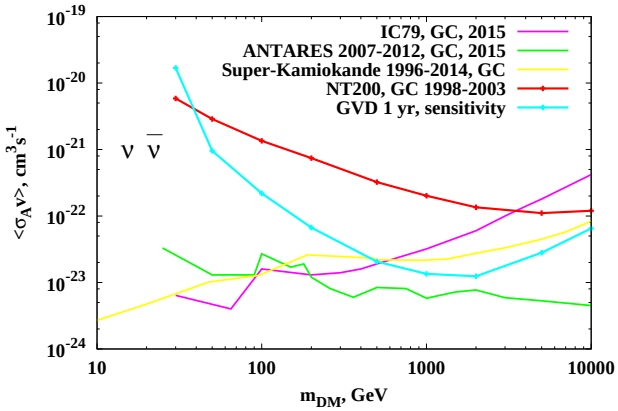

Figure 10: 90% CL upper limits on dark matter annihilation cross section for $\nu\bar{\nu}$ channel obtained with NT200 dataset (red line) in this study in comparison with results from ANTARES [14], IceCube [15] and Super-Kamiokande [16] as well as with sensitivity of 12 clusters of Baikal-GVD project [27].

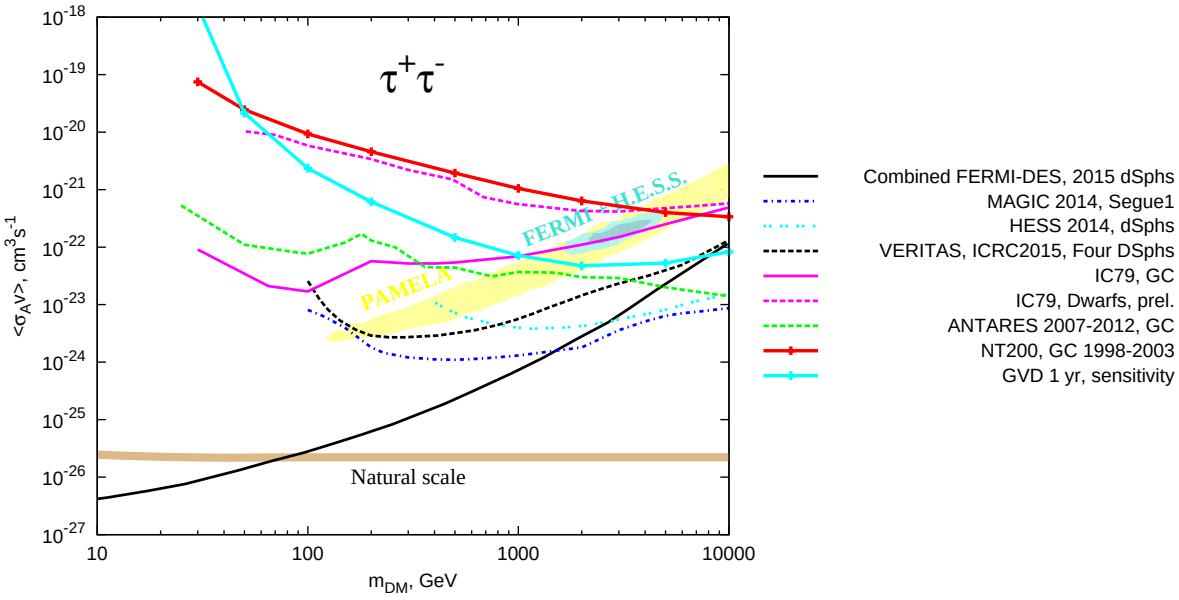

Figure 11: 90% CL upper limits on dark matter annihilation cross section for $\tau^+\tau^-$ channels obtained from NT200 data in this study in comparison with results.

preliminary results for dwarf galaxies), ANTARES [14] (GC) and 1 year sensitivity of Baikal-GVD (GC) [21]. Colorful regions show the results of DM interpretation [54] of positron excess observed by PAMELA [55] combined with FERMI [56] and HESS [57] data. Light brown line shows the thermal relic annihilation cross section from Ref. [58].

Let us further discuss the systematic uncertainties. They include both experimental and theoretical parts. The uncertainties in the optical properties of water and in the sensitivity of the optical modules result in 30% experimental uncertainty [23, 26]. Theoretical uncertainties include present errors in oscillation parameters and uncertainty in neutrino-nucleon cross section. They have been estimated using procedure described

in [27] and reach 10-12% depending on annihilation channel. We include the above uncertainties when presenting the upper limits. However, the main uncertainty comes from astrophysics. To illustrate this we carry out new analysis using the method A with Burkert and Moore dark matter density profiles for monochromatic neutrino annihilation channels: we make new MC simulation of the signal events and obtain new values of optimized cones. In Fig. 12 we show for illustration expected reconstructed muon angular

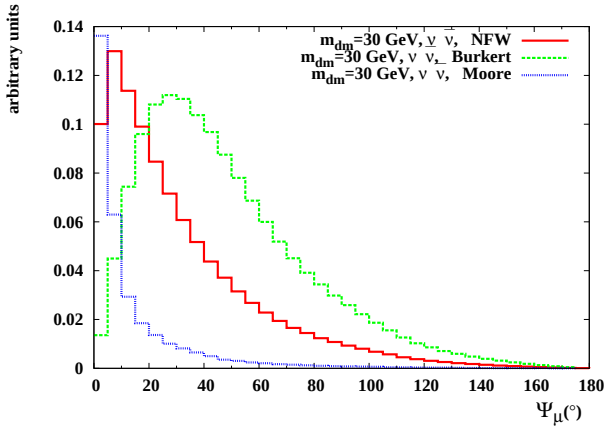

Figure 12: Reconstructed muon angular distribution from dark matter annihilation over $\nu\bar{\nu}$ channels for different dark matter density profiles. Relative normalizations are scaled for convenience of presentation.

distribution from this signal for $\nu\bar{\nu}$ annihilation channels for different dark matter density profiles. Using optimization procedure we found that for Burkert profile the cone half-angle should be about $56-57^\circ$ while for Moore profile we obtain values in the range $3-11^\circ$ depending on mass of dark matter particle and annihilation channel. Corresponding integrated J_a-factors as function of cone size are shown in Fig. 13 for

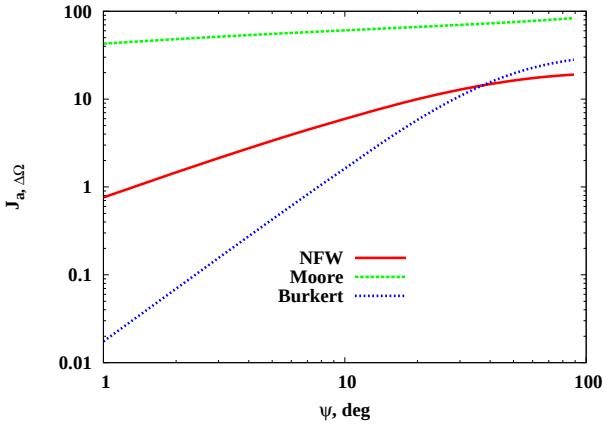

Figure 13: $J_{a,\Delta\Omega}$ as a function of cone half-angle ψ for different matter density profiles of the Milky Way.

chosen dark matter density profiles. The results for upper limits on annihilation cross section are presented in Fig. 14. We see that for very cuspy Moore profile the bounds on annihilation cross section are improved by order of magnitude: this is related to considerably larger values of J_a-factors even for very small opening angles as compared to NFW profile. At the same time cored Burkert profile results in almost the same upper limits: in this case large background from new opening angle is compensated by larger astrophysical factor: we see that J_a for the case of Burkert profile is larger than for NFW at $\psi \gtrsim 37^\circ$. Finally, let us mention the

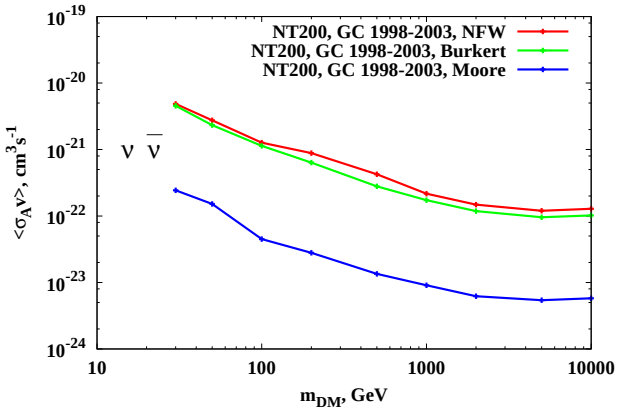

Figure 14: 90% CL upper limits on dark matter annihilation cross section for $\nu\bar{\nu}$ channel obtained from NT200 data in this study for different profiles of dark matter density in the Milky Way.

uncertainty in J_a-factor related to a possible asphericity of dark matter halo [59] which can reach values up to 35%.

6. Conclusions

To summarize, we have studied the NT200 response to neutrinos from dark matter annihilations in the Galactic Center. We perform two independent analyses looking for an excess of neutrino events towards the GC. Both analyses show similar results. The upper limits on dark matter annihilation cross section for 2.76 live years of observation reach values of about 10^{-22} cm^{3}s^{-1} at 90% CL in channel of $\nu\bar{\nu}$ pairs when a mass of dark matter particles is heavier than 5 TeV.

Acknowledgments

The work of S.V. Demidov and O.V. Suvorova was supported by the RSCF grant 14-12-01430.

References

[1] M. Persic, P. Salucci and F. Stel, "The Universal rotation curve of spiral galaxies: 1. The Dark matter connection," Mon. Not. Roy. Astron. Soc. **281** (1996) 27, [astro-ph/9506004].
[2] D. Clowe et al., "On dark peaks and missing mass: a weak-lensing mass reconstruction of the merging cluster system A520," ApJ 758, p 128, 2012.
[3] Spergel, D. N., Verde, L., Peiris, H. V. et al., "First Year Wilkinson Microwave Anisotropy Probe (WMAP) Observations: Determination of Cosmological Parameters," ApJS, 148, 175, 2003, arXiv:astro-ph/0302209.
[4] Hinshaw, G., Larson, D., Komatsu, E., et al., "Nine-Year Wilkinson Microwave Anisotropy Probe (WMAP) Observations: Cosmological Parameter Results," 2012, arXiv:1212.5226.
[5] Planck collaboration, P. A. R. Ade et al., "Planck 2013 results. XV. CMB power spectra and likelihood," 2013, arXiv:1303.5075.
[6] J. R. Primack, "Dark matter and structure formation," astro-ph/9707285.
[7] K. Jedamzik and M. Pospelov, "Big Bang Nucleosynthesis and Particle Dark Matter," New J. Phys. **11** (2009) 105028, [arXiv:0906.2087 [hep-ph]].
[8] G. Bertone, D. Hooper and J. Silk, "Particle dark matter: Evidence, candidates and constraints," Phys. Rept. **405** (2005) 279 [hep-ph/0404175].
[9] G. Steigman and M. S. Turner, "Cosmological Constraints on the Properties of Weakly Interacting Massive Particles," Nucl. Phys. B **253** (1985) 375.
[10] G. Jungman, M. Kamionkowski and K. Griest, "Supersymmetric dark matter," Phys. Rept. **267** (1996) 195, [hep-ph/9506380].

[11] D. Hooper and S. Profumo, "Dark matter and collider phenomenology of universal extra dimensions," Phys. Rept. **453** (2007) 29 [hep-ph/0701197].
[12] Daylan T., Finkbeiner D.P., Hooper D., Linden T., Portillo S.K.N., Rodd N.L., Slatyer T.R., "The Characterization of the Gamma-Ray Signal from the Central Milky Way: A Compelling Case for Annihilating Dark Matter", FERMILAB-PUB-14-032-A. (2014) arXiv. 1402.6703.
[13] Ackerman M. et al. [FERMI-LAT Collab.] "Limits on Dark Matter Annihilation Signals from the Fermi LAT 4-year Measurement of the Isotropic Gamma-Ray Background", (2015). arXiv. 1501.05464.
[14] S. Adrian-Martinez *et al.* [ANTARES Collaboration], "Search of Dark Matter Annihilation in the Galactic Centre using the ANTARES Neutrino Telescope," JCAP **1510** (2015) 10, 068, [arXiv:1505.04866 [astro-ph.HE]].
[15] M. G. Aartsen *et al.* [IceCube Collaboration], "Search for Dark Matter Annihilation in the Galactic Center with IceCube-79," Eur. Phys. J. C **75** (2015) 10, 492, [arXiv:1505.07259 [astro-ph.HE]].
[16] K. Frankiewicz [Super-Kamiokande Collaboration], "Searching for Dark Matter Annihilation into Neutrinos with Super-Kamiokande," arXiv:1510.07999 [hep-ex].
[17] I.A. Belolaptikov et al., [Baikal Collab.], "The Baikal underwater neutrino telescope: Design, performance and first results", Astropart.Phys. 7 (1997) 263-282.
[18] V.M. Aynutdinov et al., [Baikal Collab.], "Baikal neutrino telescope", Phys.Atom.Nucl. 69 (2006) 1914-1921.
[19] A. D.Avrorin et al., [Baikal Collab.], "Baikal-GVD: first cluster Dubna", PoS EPS-HEP2015 (2015), arXiv:1511.02324[physics.ins-det].
[20] A. D.Avrorin et al.,[Baikal Collab.], "Status and recent results of the BAIKAL-GVD project", Phys. Part. Nucl. 46 (2015) 2, 211-221.
[21] A. D.Avrorin et al., [Baikal Collab.], "Sensitivity of the Baikal-GVD neutrino telescope to neutrino emission toward the center of the galactic dark matter halo", JETP Lett. 101 (2015) 5, 289-294, arXiv:1412.3672 [astro-ph.HE].
[22] V. Aynutdinov et al., [Baikal Collab.], "The Baikal Neutrino experiment: Status, selected physics results, and perspectives," Izvestia Akademii Nauk (Izvestia Russ. Academy Science), Ser. Phys., vol. 71, N. 4, 2007.
[23] V.M. Aynutdinov et al., [Baikal Collab.], "Search for relativistic magnetic monopoles with the Baikal Neutrino Telescope", Astropart.Phys. 29 (2008) 366-372.
[24] V. Aynutdinov et al.,[Baikal Collab.], "The BAIKAL neutrino experiment: Physics results and perspectives," Nucl. Instrum. Methods, vol A602, p 14, 2009.
[25] A.V. Avrorin et al., [Baikal Collab.], "Search for neutrinos from Gamma-Ray Bursts with the Baikal Neutrino Telescope NT200", Astronomy Lett. V.37, N.10 (2011) 692-698.
[26] A.V. Avrorin et al., [Baikal Collab.], "Search for astrophysical neutrinos in the Baikal neutrino project", Phys.Part.Nucl.Lett. 8 (2011) 704-716.
[27] A. D. Avrorin *et al.* [Baikal Collaboration], 'Search for neutrino emission from relic dark matter in the Sun with the Baikal NT200 detector," Astropart. Phys. **62** (2014) 12, [arXiv:1405.3551 [astro-ph.HE]].
[28] D. Heck et al., Forschungszemtrum Karlsruhe, Technical Report No. 6019, 1998.
[29] E. Bugaev, S. Klimushin, I. Sokalsky, Phys. Rev. D, vol. 64, p. 074015, 2001.
[30] V. Agrawal, T. Gaisser, P. Lipari and T. Stanev, "Atmospheric neutrino flux above 1 GeV," Phys. Rev., vol. D53, p. 1314, 1996.
[31] I. A. Belolaptikov, Preprint of INR RAS 1178/2007 (in Russian), 2007.
[32] J. F. Navarro, C. S. Frenk and S. D. M. White, Astrophys. J. **462** (1996) 563.
[33] J. F. Navarro, C. S. Frenk and S. D. M. White, Astrophys. J. **490** (1997) 493
[34] A. V. Kravtsov, A. A. Klypin, J. S. Bullock and J. R. Primack, Astrophys. J. **502** (1998) 48
[35] B. Moore, S. Ghigna, F. Governato, G. Lake, T. R. Quinn, J. Stadel and P. Tozzi, Astrophys. J. **524** (1999) L19
[36] A. Burkert, IAU Symp. **171** (1996) 175 [Astrophys. J. **447** (1995) L25.
[37] M. Kuhlen, M. Vogelsberger and R. Angulo, Phys. Dark Univ. **1** (2012) 50 doi:10.1016/j.dark.2012.10.002 [arXiv:1209.5745 [astro-ph.CO]].
[38] V. S. Berezinsky, V. I. Dokuchaev and Y. N. Eroshenko, Phys. Usp. **57** (2014) 1 [Usp. Fiz. Nauk **184** (2014) 3] doi:10.3367/UFNe.0184.201401a.0003 [arXiv:1405.2204 [astro-ph.HE]].
[39] P. Baratella, M. Cirelli, A. Hektor, J. Pata, M. Piibeleht and A. Strumia, "PPPC 4 DMν: A Poor Particle Physicist Cookbook for Neutrinos from DM annihilations in the Sun," arXiv:1312.6408 [hep-ph].
[40] D. V. Forero, M. Tortola and J. W. F. Valle, "Neutrino oscillations refitted," Phys. Rev. D **90** (2014) 093006, [arXiv:1405.7540 [hep-ph]].
[41] M. M. Boliev, S. V. Demidov, S. P. Mikheyev and O. V. Suvorova, "Search for muon signal from dark matter annihilations in the Sun with the Baksan Underground Scintillator Telescope for 24.12 years," JCAP **1309** (2013) 019, [arXiv:1301.1138 [astro-ph.HE]].
[42] G. C. Hill and K. Rawlins, "Unbiased cut selection for optimal upper limits in neutrino detectors: The Model rejection potential technique," Astropart. Phys. **19** (2003) 393, [astro-ph/0209350].
[43] Wolfgang A. Rolke, Angel M. Lopez, Jan Conrad, "Limits and confidence intervals in the presence of nuisance parameters," Nucl.Instrum.Meth. **A551** (2005) 493-503
[44] http://root.cern.ch R. Brun et al., Nucl. Instrum. Methods in Phys. Res., 1996
[45] S. S. Wilks, "The Large-Sample Distribution of the Likelihood Ratio for Testing Composite Hypotheses," Annals Math. Statist. **9** (1938) 1, 60. doi:10.1214/aoms/1177732360
[46] K. A. Olive *et al.* [Particle Data Group Collaboration], "Review of Particle Physics," Chin. Phys. C **38** (2014) 090001.
[47] A. Cooper-Sarkar, P. Mertsch and S. Sarkar, "The high energy neutrino cross-section in the Standard Model and its uncertainty," JHEP **1108** (2011) 042, [arXiv:1106.3723 [hep-ph]].

[48] R. Catena and P. Ullio, "A novel determination of the local dark matter density," JCAP **1008** (2010) 004 [arXiv:0907.0018 [astro-ph.CO]].
[49] A. Drlica-Wagner *et al.* [Fermi-LAT and DES Collaborations], "Search for Gamma-Ray Emission from DES Dwarf Spheroidal Galaxy Candidates with Fermi-LAT Data," Astrophys. J. **809** (2015) 1, L4 [arXiv:1503.02632 [astro-ph.HE]].
[50] B. Zitzer [VERITAS Collaboration], 'Search for Dark Matter from Dwarf Galaxies using VERITAS," arXiv:1509.01105 [astro-ph.HE].
[51] J. Aleksic *et al.*, "Optimized dark matter searches in deep observations of Segue 1 with MAGIC," JCAP **1402** (2014) 008, [arXiv:1312.1535 [hep-ph]].
[52] A. Abramowski *et al.* [HESS Collaboration], "Search for dark matter annihilation signatures in H.E.S.S. observations of Dwarf Spheroidal Galaxies," Phys. Rev. D **90** (2014) 112012, [arXiv:1410.2589 [astro-ph.HE]].
[53] M. G. Aartsen *et al.* [IceCube Collaboration], "The IceCube Neutrino Observatory - Contributions to ICRC 2015 Part IV: Searches for Dark Matter and Exotic Particles," arXiv:1510.05226 [astro-ph.HE].
[54] P. Meade, M. Papucci, A. Strumia and T. Volansky, Nucl. Phys. B **831** (2010) 178 [arXiv:0905.0480 [hep-ph]].
[55] O. Adriani *et al.* [PAMELA Collaboration], Nature **458** (2009) 607 doi:10.1038/nature07942 [arXiv:0810.4995 [astro-ph]].
[56] A. A. Abdo *et al.* [Fermi-LAT Collaboration], Phys. Rev. Lett. **102** (2009) 181101 doi:10.1103/PhysRevLett.102.181101 [arXiv:0905.0025 [astro-ph.HE]].
[57] F. Aharonian *et al.* [HESS Collaboration], Phys. Rev. Lett. **101** (2008) 261104 doi:10.1103/PhysRevLett.101.261104 [arXiv:0811.3894 [astro-ph]].
[58] G. Steigman, B. Dasgupta and J. F. Beacom, "Precise Relic WIMP Abundance and its Impact on Searches for Dark Matter Annihilation," Phys. Rev. D **86** (2012) 023506, [arXiv:1204.3622 [hep-ph]].
[59] N. Bernal, J. E. Forero-Romero, R. Garani and S. Palomares-Ruiz, "Systematic uncertainties from halo asphericity in dark matter searches," JCAP **1409** (2014) 004 doi:10.1088/1475-7516/2014/09/004, [arXiv:1405.6240 [astro-ph.CO]].